Gap Junction Dynamics: Reversible Effects of Divalent Cations

CAMILLO PERACCHIA and LILLIAN L. PERACCHIA
Department of Physiology, University of Rochester, School of Medicine and Dentistry, Rochester, New York 14642

ABSTRACT Reversible changes in gap junction structure similar to those previously seen to parallel electrical uncoupling (9, 33, 34) are produced by treating with Ca^{++} or Mg^{++} gap junctions isolated in EDTA from calf lens fibers. The changes, characterized primarily by a switch from disordered to crystalline particle packings, occur at a $[Ca^{++}]$ of $5 \cdot 10^{-7}$ M or higher and a $[Mg^{++}]$ of $1 \cdot 10^{-3}$ M or higher and can be reversed by exposing the junctions to Ca^{++}- and Mg^{++}-free EGTA solutions. Similar changes are obtained in junctions of rat stomach epithelia incubated at 37°C in well-oxygenated Tyrode's solutions containing a Ca^{++} ionophore (A23187). Deep etching experiments on isolated lens junctions show that the true cytoplasmic surface of the junctions (PS face) is mostly bare, suggesting that the particles may not be connected to cytoskeletal elements. A hypothesis is proposed suggesting a mechanism of particle aggregation and channel narrowing based on neutralization of negative charges by divalent cations or H^+.

Cell uncoupling is a phenomenon by which neighboring cells capable of directly exchanging small protoplasmic molecules lose their communicating property to become independent from each other. Loss of intercellular coupling is believed to follow the occlusion of intercellular channels generally thought to be at the intramembrane particles of gap junctions (31).

After uncoupling treatments, changes in the structure of gap junctions have been described. These changes, characterized by an increase in tightness and crystallinity of the particle packings, a decrease in particle diameter, and in one case (33, 34) a decrease in gap thickness, have been interpreted to reflect modifications in gap junction proteins resulting in channel occlusion (1, 2, 27, 28, 33, 34). However, direct correlation between functional uncoupling and gap junction crystallinity has been demonstrated in only two studies (9, 33, 34).

Little is known about the molecular mechanisms that modulate the junctional permeability, but some data on the factors which trigger uncoupling are available. A number of studies have supported a close correlation between cell uncoupling and an increase in cytoplasmic free calcium $[Ca^{++}]_i$ (10–13, 21, 22, 24, 39, 40) or other divalent cations (13, 14, 24, 38). Recently, a monovalent cation, H^+, has also been thought to affect coupling independently from Ca^{++} (17, 18, 42, 43, 44).

To learn whether or not divalent cations and H^+ affect gap junction permeability by acting directly on gap junction macromolecules, and whether or not the structural changes seen in gap junctions of cells exposed to uncoupling treatments are indeed part of the uncoupling mechanism, epithelial cells of rat stomach have been exposed to a calcium ionophore and isolated calf lens junctions have been treated with buffered solutions of increasing Ca^{++}, Mg^{++}, or H^+ concentration. Preliminary experiments on isolated lens junctions have shown that these ions affect the gap junction structure independently; namely, incubation of the junctions in solutions with a $[Ca^{++}]$ of $5 \cdot 10^{-7}$ M or higher (29, 30), a $[Mg^{++}] > 1 \cdot 10^{-3}$ M (31, 32), and a $[H^+]$ of $3 \cdot 10^{-7}$ M or higher (36, 37) caused the junctional particles to aggregate tightly into crystalline arrays similar to those seen after uncoupling treatments. Gap junction crystallization could also be induced in intact lens fibers by treatments which increase the intracellular calcium content (32).

This paper concerns the reversible effects of divalent cations, while the companion paper (37) deals with the effects of hydrogen ions.

MATERIALS AND METHODS

Rat Stomach: Effects of a Calcium Ionophore

1- to 2-mo-old rats (Charles River Breeding Laboratories, Inc., Wilmington, Mass.) were sacrificed by brain concussion. Specimens of ~0.5 cm^2 were cut from the stomach body and incubated for 1 h at 37°C in well oxygenated Tyrode's solutions containing $2 \cdot 10^{-6}$ M A23187 calcium ionophore (Eli Lilly and Company, Indianapolis, Ind.). As a control, specimens from the same stomach were incubated similarly in Tyrode's solutions lacking the ionophore. All the samples

THE JOURNAL OF CELL BIOLOGY · VOLUME 87 DECEMBER 1980 708-718
© The Rockefeller University Press · 0021-9525/80/12/0708/11 $1.00

were fixed for 90 min with a 3% glutaraldehyde-H_2O_2 solution (35) buffered to pH 7.4 with 0.1 M sodium cacodylate at room temperature and freeze-fractured (28) with a Denton freeze-fracture device (Denton Vacuum, Inc., Cherry Hill, N. J.) after treatment with a 10, 20, 30% series of glycerol solutions in H_2O at 15–30-min intervals.

The composition of the normal Tyrode's solution (in millimoles/liter) was: $CaCl_2$, 1.8; $MgCl_2$, 0.49; KCl, 5; $NaHCO_3$, 11.9; NaCl, 137; NaH_2PO_4, 0.362; glucose, 5.6; pH 7.3. The solution of A23187 ionophore was prepared as follows: 10 mg of A23187 (523, mol wt) were dissolved in 20 ml of chloroform containing 40 mg of polyvinylpyrrolidone (PVP). After vacuum evaporation of chloroform, the solid product was dissolved in water to obtain a 100-mg/ml concentration of A23187. This stock solution was stored at −20°C. Before each experiment this solution was diluted 1:100 in Tyrode's solution to reach the final ionophore concentration of $2 \cdot 10^{-6}$ M.

In junctions with crystalline arrays, the average center-to-center spacing between adjacent particles or pits was obtained by measuring the mean particle periodicity along each of three rows of particles or pits oriented along axes at 120° to each other and by calculating the average of the three means (28). In junctions with disordered arrays, equal numbers of center-to-center spacing between neighboring particles or pits were measured along three axes at 120° to each other and the average spacing was calculated (28).

Calf Eye Lens: Effects of Divalent Cations on Isolated Junctions

ISOLATION OF CRUDE GAP JUNCTION FRACTION: Ten lenses per experiment were dissected from the posterior wall of calf eyes (Conti Packing Co., Inc., Henrietta, N. Y.) 30–45 min after the animal death. The lenses were immersed in $3 \cdot 10^{-3}$ M EDTA (Eastman Kodak Corp., Rochester, N. Y.) solutions buffered to pH 7.4 with $1 \cdot 10^{-3}$ M sodium bicarbonate, minced, and rapidly homogenized (5 lenses/25 ml of solution) for 15 s at 4°C with a Tekmar Tissumizer Model SDT 100 N (Tekmar Co., Cincinnati, Ohio) set at 15,000 rpm. The homogenate was diluted two fold with EDTA-bicarbonate buffer, filtered through four layers of cheese cloth and centrifuged for 10 min at 1,500 *g* with a Sorval RC2-B centrifuge (I. Sorval Inc., Norwalk, Conn.). The pellet was washed four times by suspending it in EDTA-bicarbonate buffer and centrifuging it at 1,500, 1,200, and 17,000 *g*, respectively. The final pellet was stored at −20°C for periods not exceeding 2 wk.

CALCIUM EFFECTS: Pellets of crude junction fractions isolated as described above were washed by mild homogenization with a Dounce homogenizer (three strokes) in solutions in which the concentration of ionized calcium $[Ca^{++}]$ was buffered to values ranging from $1 \cdot 10^{-7}$ to $1 \cdot 10^{-5}$ M with $1 \cdot 10^{-2}$ M EDTA and the pH to 7 with $2 \cdot 10^{-2}$ M 4-(2-hydroxylethyl)-1-piperazimethane sulfonic acid (Hepes) (Sigma Chemical Co., St. Louis, MO.). The suspensions were centrifuged for 30 min at 27,000 *g* and the pellets were resuspended and incubated in the same solutions for 30 min at 37°C after mild homogenization (20 strokes) with a Dounce homogenizer. At the end of the incubation period the junctions were fixed by mixing the suspensions 1:1 with 6% glutaraldehyde solutions buffered to pH 7.4 with 0.2 M sodium cacodylate. After 15–20 min; the suspensions were centrifuged for 30 min at 27,000 *g*, and the pellets treated with 30% glycerol and freeze-fractured either with a Denton freeze-fracture device or a Balzers BAF 301 freeze-etch unit (Balzers High Vacuum Corp., Santa Ana, Calif.). Control samples were treated similarly with Ca^{++}- and Mg^{++}-free EDTA-Hepes solutions.

The calcium buffered solutions were prepared by dissolving calculated amounts of $CaCl_2$ into $1 \cdot 10^{-2}$ M solutions of EDTA buffered to pH 7 with $2 \cdot 10^{-2}$ M Hepes. $CaCl_2$ was added by dilution from 1 M stock solutions. The amounts of $CaCl_2$ to be added were calculated using an EDTA dissociation constant for calcium of $5 \cdot 10^{-4}$ M (at pH 7, log K = 7.3) (7). The following equation was used:

$$[Ca^{++}]_f = ([Ca^{++}]_f\,[EDTA]_f + [Ca^{++}]_f^2 + [Ca^{++}]_f\,K_D)/(K_D + [Ca^{++}]_f), \quad (1)$$

where $[Ca^{++}]_f$ represents the amount of total calcium per unit volume of medium, which gives a concentration of free calcium $[Ca^{++}]_f$, when the total amount of EDTA per unit volume of medium is $[EDTA]_f$, and K_D is the dissociation constant of the reaction: Ca + EDTA ⇌ CaEDTA. The dissociation curves for Ca- and Mg-EDTA at pH 7 are shown in Fig. 1.

MAGNESIUM EFFECTS: Pellets of crude junction fractions, isolated as described above, were washed and subsequently incubated (see above) in solutions in which the ionized magnesium $[Mg^{++}]$ was set at values ranging from $1 \cdot 10^{-6}$ to $5 \cdot 10^{-3}$ M. For $[Mg^{++}]$ ranging from $1 \cdot 10^{-6}$ to $1 \cdot 10^{-4}$ M, $1 \cdot 10^{-2}$ M EDTA was used, while for $[Mg^{++}]$ or $1 \cdot 10^{-3}$ M and higher, the EDTA was $5 \cdot 10^{-2}$ M. The solutions were buffered to pH 7 with $2 \cdot 10^{-2}$ M Hepes. The amounts of $MgCl_2$ to be added were calculated using an EDTA dissociation constant for magnesium of $4 \cdot 10^{-6}$ M (at pH 7, log K = 5.4) (7) and the same equation used for calcium (see above).

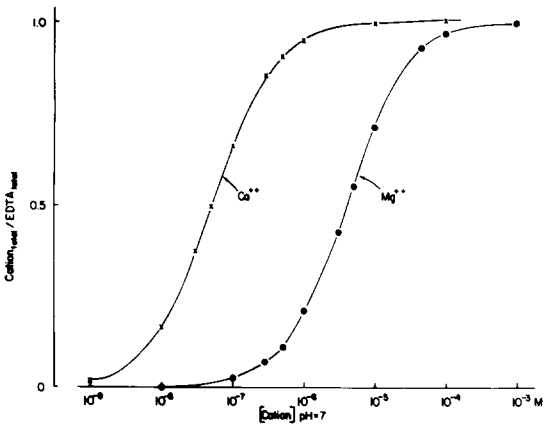

FIGURE 1 Relationship between $[Ca^{++}]$ or $[Mg^{++}]$ (on the abscissa) and Ca or Mg total/EDTA total (on the ordinate) at pH 7, calculated using an EDTA dissociation constant of $5 \cdot 10^{-8}$ M (for Ca) and $4 \cdot 10^{-7}$ M (for Mg).

In other experiments the junctions were washed and incubated in solutions containing $3 \cdot 10^{-3}$ M EGTA (Sigma), $2 \cdot 10^{-2}$ M Hepes, pH 7, and $MgCl_2$ (added by dilution from a 1 M solution) to obtain a final $[Mg^{++}]$ of $1 \cdot 10^{-3}$, $1 \cdot 10^{-4}$, and $1 \cdot 10^{-5}$ M. At the end of the incubation period the suspensions were fixed, centrifuged, and freeze-fractured as described above. Some of the pellets from glutaraldehyde-fixed. Mg^{++}-treated junctions were freeze-fractured without cryoprotective treatment and etched for 4 min at −105°C to expose the cytoplasmic surface of the junctions.

ROLE OF ENDOGENOUS ATP: To test whether or not endogenous ATP, possibly present in the preliminary crude junction fractions, is necessary for the occurrence of calcium-magnesium effects on isolated gap junctions, pellets from crude junction fractions isolated as described above were suspended and incubated for 30 min at 37°C in solutions containing 15 U/ml of hexokinase (type F-300, Sigma), $5 \cdot 10^{-3}$ M glucose, $5 \cdot 10^{-4}$ M $MgCl_2$, $3 \cdot 10^{-3}$ M EGTA, and $2 \cdot 10^{-2}$ M Tris-HCl, pH 7.4. At the end of the incubation period the suspensions were divided into two samples. Sample 1 was fixed, centrifuged, and freeze-fractured as previously described. Sample 2 was washed and subsequently incubated for 30 min at 37°C in a solution containing $1 \cdot 10^{-3}$ M $MgCl_2$, $3 \cdot 10^{-3}$ M EGTA, $2 \cdot 10^{-2}$ M Hepes, pH 7, and the necessary amount of $CaCl_2$ to obtain a final $[Ca^{++}]$ of $1 \cdot 10^{-5}$ M. The amount of $CaCl_2$ to be added was calculated using Eq. 1 and an EGTA dissociation constant for calcium (at pH 7) of $2.04 \cdot 10^{-7}$ M (45). At the end of the incubation period the suspension was fixed, centrifuged, and freeze-fractured as described above.

ATP ASSAY: The ATP content of either untreated or hexokinase-treated pellets from crude junction preparations was determined using the hexokinase, glucose-6-phosphate dehydrogenase method (19).

RECOVERY EXPERIMENTS: Pellets of crude junction fractions, isolated as described above, were washed and incubated as above in solutions containing $3 \cdot 10^{-3}$ M EGTA, $2 \cdot 10^{-2}$ M Hepes, pH 7, $1 \cdot 10^{-3}$ M $MgCl_2$, and enough $CaCl_2$ to reach a final $[Ca^{++}]$ of $1 \cdot 10^{-4}$ M. The amount of $CaCl_2$ to be added was calculated as described above. At the end of the incubation period the specimen was divided into two samples. Sample 1 was fixed, centrifuged, and freeze-fractured as previously described. Sample 2 was washed and subsequently incubated for 30 min at 37°C in a recovery solution containing $3 \cdot 10^{-3}$ M EGTA and $2 \cdot 10^{-2}$ M Tris-HCl, pH 7.5. In some recovery solutions, ATP (A3127, Sigma) was added to a final concentration of 1 to $7 \cdot 10^{-3}$ M. Some of the ATP solutions contained $1 \cdot 10^{-4}$ $[Mg^{++}]$. At the end of the incubation period the suspension was fixed, centrifuged, and freeze-fractured as previously described.

Electron Microscopy

The specimens were examined with an AEI EM 801 electron microscope. The microscope magnification was standardized before each photographic exposure by eliminating the hysteresis of the lenses. All the magnifications were previously standardized with a carbon grating replica (model 1002, E. F. Fullam, Inc., Schenectady, N. Y.).

In the freeze-fracture micrographs, the direction of the platinum shadowing is from the bottom up. Fracture faces and membrane surfaces have been labeled according to Branton et al. (5); P and E indicate the fracture face of protoplasmic and exoplasmic leaflets, respectively, and PS the true surface of the protoplasmic leaflet.

In freeze-fracture replicas of pellets from crude lens junction fractions, the gap junctions were identified as regions in which the fracture plane exposed the

fracture faces of two membranes closely apposed to each other, the top one displaying an aggregate of pits and the bottom an aggregate of particles. Gap junctions displaying only one of the two fracture faces were identified only when both face- and cross-views of the same junction were seen, such that the profile of two membranes closely apposed to each other at the junction and separated from each other at perijunctional regions could be clearly recognized.

RESULTS

Stomach

Gap junctions between epithelial cells of rat stomach kept for 1 h in well-oxygenated Tyrode's solution at 37°C display in freeze-fracture the typical appearance of control junctions (28), characterized by disorderly packed arrays of particles (Fig. 2) spaced, most often, at an average center-to-center distance of 10.5 nm (Fig. 7). On the contrary, in specimens from the same stomach similarly incubated in Tyrode's solutions containing $2 \cdot 10^{-6}$ M calcium ionophore, the epithelial gap junctions most often display regularly hexagonal particle packings (Figs. 3 and 4) with an average unit cell dimension of 8.5 nm (Fig. 7). Differently from hexagonal packings previously seen in gap junctions of stomach epithelium treated with different uncoupling procedures (28), the crystalline particle packings of ionophore treated junctions are most often subdivided into small domains separated from each other by particle-free isles (Figs.

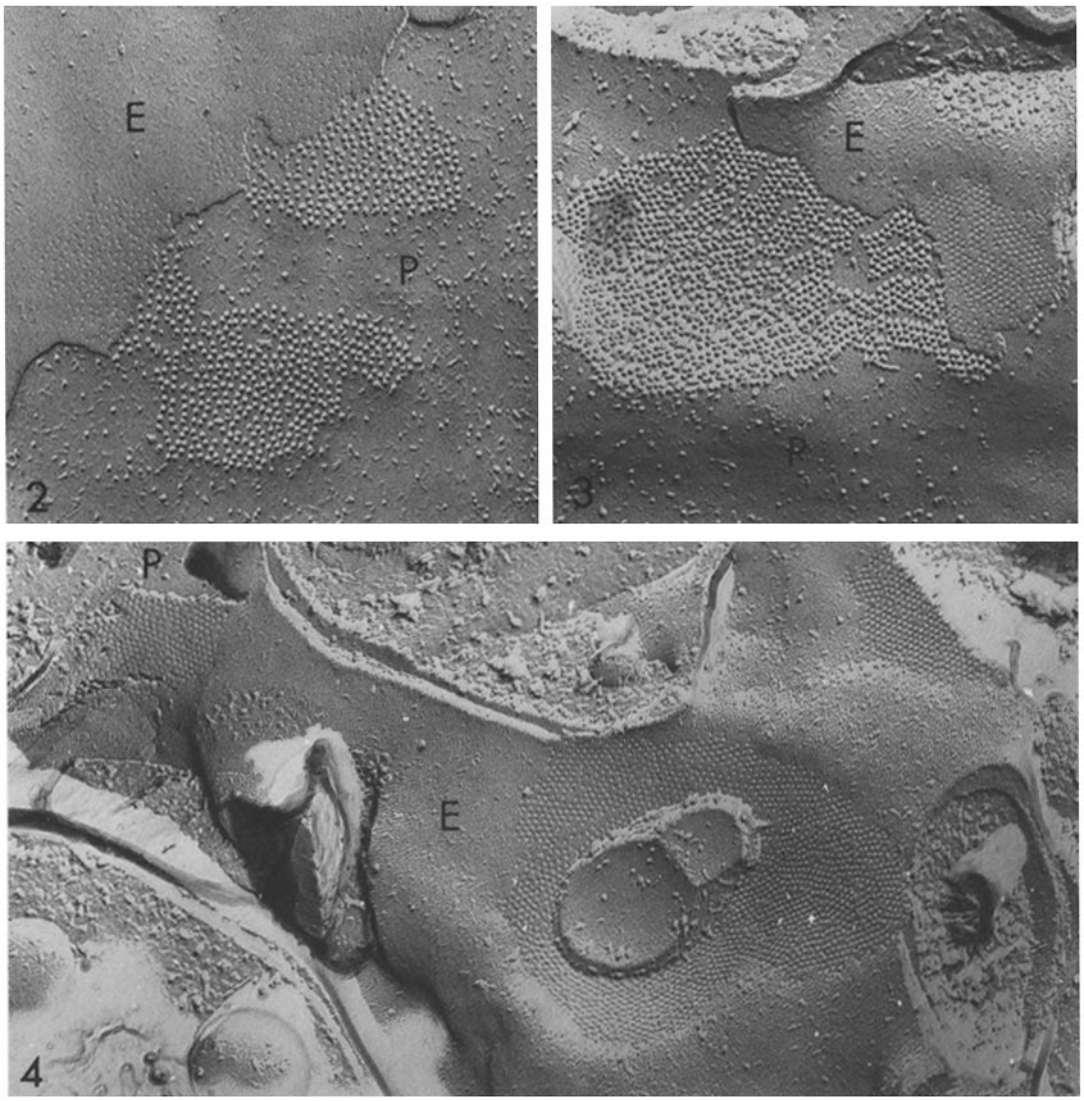

FIGURE 2 Freeze-fracture replica of a control gap junction from the epithelium of rat stomach fixed after a 1-h incubation in a well oxygenated Tyrode's solution at 37°C. The fracture plane steps down from E face (*E*) to P face (*P*). Notice that particles and complimentary pits are irregularly packed. × 103,000.

FIGURE 3 Freeze-fracture replica of a gap junction from the epithelium of rat stomach fixed after a 1-h incubation at 37°C in a well oxygenated Tyrode's solution containing $2 \cdot 10^{-6}$ M calcium ionophore (A23187). Particles on P face (*P*) and pits on E face (*E*) are hexagonally packed into small crystalline domains separated by particle free isles. The average center-to-center distance between neighboring particles or pits is 8.5 nm. × 103,000.

FIGURE 4 Freeze-fracture replica or gap junctions from a stomach sample treated as described in Fig. 3. E face (*E*) pits form crystalline domains oriented at various angles. A cytoplasmic membrane of undetermined nature is closely apposed to the membrane of the larger gap junction. Close association between gap junctions and cytoplasmic membranes is seen more frequently in junctions with crystalline particle packings. *P*, P face. × 103,000.

3 and 4). Frequently observed in crystalline junctions are also fragments of cytoplasmic membranes closely apposed to gap junction surfaces (Fig. 4).

Fig. 5 shows the E face of an ionophore treated gap junction which has been cleaved in an unusual manner. The path followed by the fracture plane is represented diagramatically in Fig. 6, which shows the profile of that region of Fig. 5 comprised between the two arrows. Following the direction of the arrows (Fig. 5) from the bottom up, the fracture plane first exposes a number of gap junction pits, then moves into the cytoplasm (*Ct*) and eventually returns into a nonjunctional membrane region (E face). Where the fracture plane enters the cytoplasm, one can see a row of gap junction particles exposed on their cytoplasmic end. Noteworthy is that the cytoplasmic medium surrounding the particle protrusions is rather smooth and unstructured indicating that these junctional particles may not be linked to microfilaments or other elements of the cytoskeleton, as demonstrated in other gap junctions during the interiorization process (20).

Lens

CALCIUM EFFECTS: Most of the gap junctions isolated from calf lens in the presence of EDTA and incubated in Ca^{++}-EDTA solutions in which the $[Ca^{++}]$ is buffered to values lower than $5 \cdot 10^{-7}$ M display, in freeze-fracture, irregularly aggregated particles and pits at a center-to-center distance ranging from 8 to 11 nm (Fig. 8). On the contrary, almost 90% (see Table I) of lens junctions isolated in the presence of EDTA and incubated in solutions of $5 \cdot 10^{-7}$ M or higher $[Ca^{++}]$ show particles and pits orderly packed into crystalline arrays (most often hexagonal) at a center-to-center spacing ranging from 6.5 to 7 nm (Fig. 9). Some of these arrays are not precisely hexagonal and could be classified as rhombic (36, 37). Orthogonal arrays, frequently seen at low pH (36, 37), are rare in junctions exposed to divalent cations. Since in most junctions the pits are more distinct than the particles, most center-to-center spacings were measured on *E* faces. In most junctions, a few particles fracture away with the exoplasmic leaflet (*E* face). This unusual fracture property has been noticed also in junctions of intact lens fibers (30).

ENERGY REQUIREMENTS: The observation that gap junction particles can be induced to crystallize by Ca^{++} in ATP-free solutions suggested that the phenomenon does not require energy. However, the possibility that endogenous ATP could be involved in the crystallization process remained. To eliminate this possibility, any endogenous ATP present was hydrolyzed by incubating EDTA-isolated junctions in hexokinase-glucose solutions before exposing them to Ca^{++}-containing solutions. ATP assays showed trace amounts of ATP in crude gap junction fractions and absence of ATP after the hexokinase-glucose incubation. In the absence of ATP, the junctional particles form crystalline arrays as usual upon exposure to Ca^{++} (Fig. 11), while junctions exposed only to hexokinase-

FIGURE 5 Freeze-fracture of a gap junction from a rat stomach incubated in the presence of a calcium ionophore (A23187). Following the direction of the arrows from the bottom up, the fracture plane exposes E face pits, then passes into the cytoplasm (*Ct*) and eventually returns in the membrane exposing the E face (*E*) of a perijunctional region. At the edge of the junction, one sees a row of gap junction particles cleaved along their cytoplasmic side. Notice that the cytoplasmic medium (*Ct*) neighboring these particles is quite smooth, indicating the absence of cytoskeletal elements in connection with gap junction particles. × 144,100.

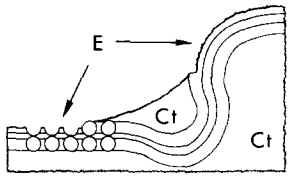

FIGURE 6 Schematic diagram of the profile of a region like the one confined between the arrows in Fig. 5, after freeze-fracture. *E*, E face; *Ct*, cytoplasm.

glucose solutions maintained disordered particle packings (Fig. 10) typical of control, EDTA-isolated junctions.

MAGNESIUM EFFECTS: Gap junctions isolated in the presence of EDTA crystallize after incubation in Ca^{++}-free solutions (pH 7) with $[Mg^{++}]$ ranging from $1 \cdot 10^{-3}$ to $5 \cdot 10^{-3}$ M. At $[Mg^{++}]$ lower than $1 \cdot 10^{-3}$ M, >95% of the junctions (Table II) display loosely and irregularly packed particle arrays typical of control junctions (Figs. 12 and 13), while at $[Mg^{++}]$ of $1 \cdot 10^{-3}$ M or greater, >80% of the junctions contain crystalline (most often hexagonal) particle packings with unit cells of 6.5–7 nm (Figs. 14–16). Interestingly, some of the junctions show regions with irregularly packed particles (Fig. 16) in direct continuity with crystalline areas. This is also observed in some junctions exposed to Ca^{++} or low pH (37). Often one sees round patches of crystallinity surrounded by disordered regions (Fig. 17), indicating that the process may develop from different nuclei of crystallization within the same junction.

RECOVERY: Junctions crystallized by incubation in solutions of $1 \cdot 10^{-4}$ M $[Ca^{++}]$ and $1 \cdot 10^{-3}$ M $[Mg^{++}]$ recover a control appearance (random particle packings) upon exposure to Ca^{++}- and Mg^{++}-free EDTA or EGTA solutions at pH 7.5. In these experiments, ~90% of the junctions (see Table III) become crystalline (Fig. 17) upon exposure to divalent cations, and ~82% of them (see Table III) assume random particle packings (Fig. 18) upon exposure to recovery solutions. Addition of 1 to $7 \cdot 10^{-3}$ M ATP with or without $1 \cdot 10^{-4}$ M $[Mg^{++}]$ does not improve the frequency of recovery.

DEEP ETCHING EXPERIMENTS: Junctions isolated in the presence of EDTA and subsequently washed and incubated in solutions of $1 \cdot 10^{-3}$ M $[Mg^{++}]$ were fixed, freeze-fractured, and deeply etched, without cryprotective treatment, to expose the true cytoplasmic surfaces (PS faces) (Figs. 19–21). These experiments were aimed at determining whether or not microfilaments or other cytoskeletal structures were intimately associated with isolated gap junction membranes. Filamentous structures are rarely seen associated with gap junction PS faces (Figs. 20 and 21). Some of the filaments (~10 nm in thickness) clearly display an axial periodicity of 5–6 nm (Fig. 21). These are probably intermediate filaments which have become associated with the junctions during the isolation procedure.

Interestingly, in deeply etched preparations junctional and nonjunctional particles appear always as very distinct units (Figs. 19 and 20). This is also observed in membranes rapidly frozen (37). In conventional freeze-fractures, however, the particles are often very distorted such that complementarity between P and E faces, especially in gap junctions, is not always obvious (Figs. 14 and 15). The lack of glycerol treatment in both the deeply etched and the rapidly frozen specimens is probably the reason for the better preservation of the particles in these preparations.

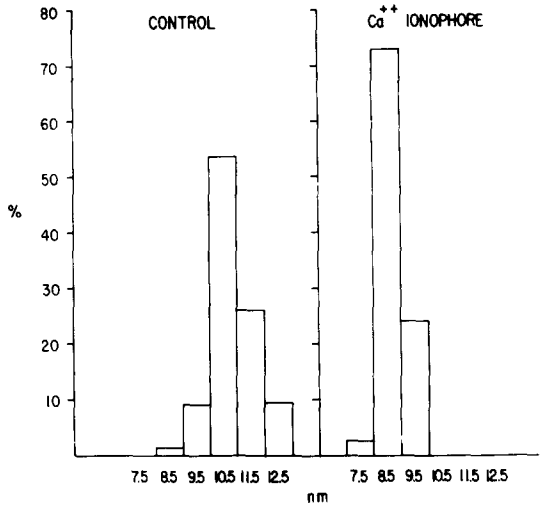

FIGURE 7 Histograms of frequencies (in percentiles) of average particle spacing measured on freeze-fractured gap junctions between epithelial cells of rat stomach. The junctions are distributed among six classes of 10 nm each. On the abscissa are the mean values of the classes. In control stomach, 53.7% of the junctions are in the 10.5 nm class (1,787 spaces were measured in 55 junctions), whereas in Ca^{++} ionophore-treated stomach, 73% are in the 8.5 nm class (770 spaces were measured in 41 junctions).

FIGURE 8 Freeze-fracture replica of a gap junction isolated from calf lens fibers, in the presence of EDTA, and subsequently incubated in a Ca-EDTA buffer in which the $[Ca^{++}]$ is $1 \cdot 10^{-7}$ M. Notice that gap junction pits are irregularly aggregated at a center-to-center distance ranging from 8 to 11 nm. Some of the pits are occupied by particles that have fractured with the exoplasmic leaflet. The arrows point to regions where the membranes join to form the gap junction. *E*, E face; *P*, P face. × 123,600.

FIGURE 9 Freeze-fracture replica of a gap junction isolated from calf lens fibers, in the presence of EDTA, and subsequently incubated in a Ca^{++} EDTA buffer in which the $[Ca^{++}]$ is $1 \cdot 10^{-6}$ M. Notice that particles and pits are packed into a crystalline array at a center-to-center spacing of 6.5–7 nm. Some of the pits are occupied by particles that have fractured away with the exoplasmic leaflet. *P*, P face; *E*, E face. × 123,600.

FIGURE 10 Freeze-fracture replica of a gap junction isolated from calf lens fibers, in the presence of EDTA, and subsequently incubated in a Ca^{++}-free, hexokinase-glucose solution to hydrolize any endogenous ATP. Notice that particles and pits are irregularly packed as in other junctions which have not been exposed to divalent cations (see Fig. 8). *P*, P face; *E*, E face. × 123,600.

FIGURE 11 Freeze-fracture replica of gap junctions isolated from calf lens fibers, in the presence of EDTA, and subsequently exposed to a Ca^{++}-free, hexokinase-glucose solution with a $[Ca^{++}]$ of $1 \cdot 10^{-5}$ M and a $[Mg^{++}]$ of $1 \cdot 10^{-3}$ M. Notice that even in absence of any endogenous ATP, exposure to divalent cations induces particles and pits to pack into crystalline arrays. *P*, P face; *E*, E face. × 123,600.

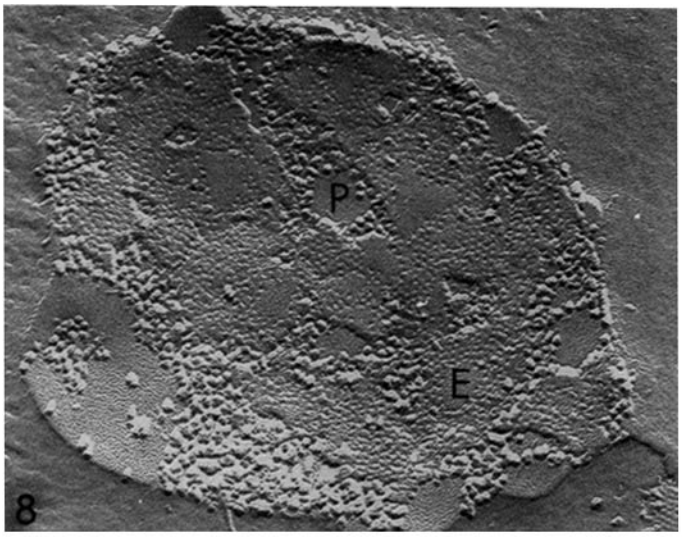
P
E
8

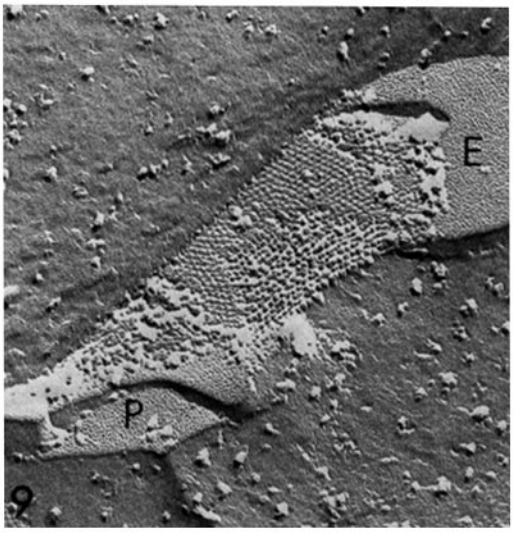
E
P
9

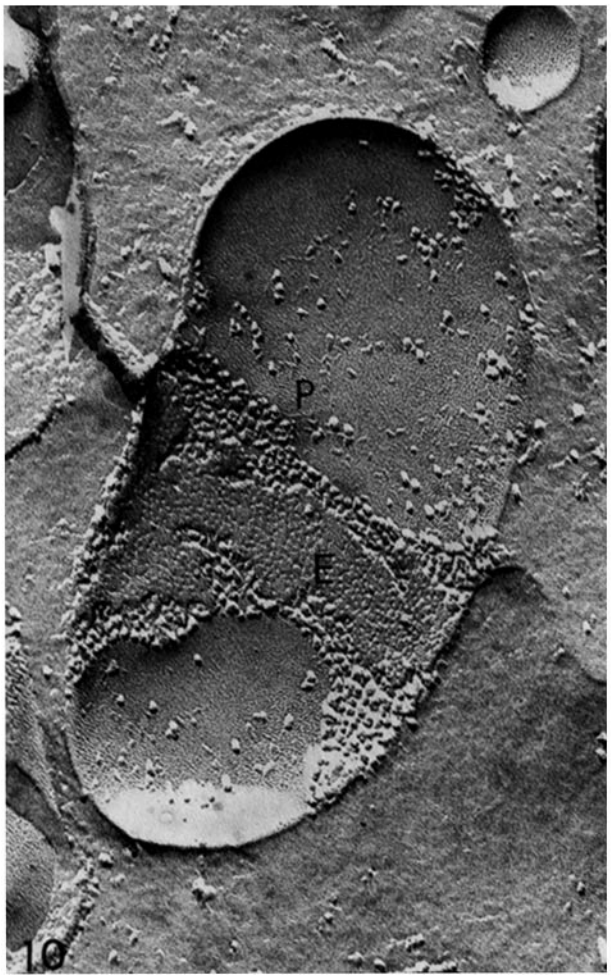
P
E
10


P
E
E
P
11

DISCUSSION

This study shows that the changes in gap junction architecture described in intact cells in parallel with electrical uncoupling (9, 33, 34) or after uncoupling treatments (1, 2, 27, 28), can be produced in isolated junctions by exposure to Ca^{++} or Mg^{++}. The changes in gap junctions are reversible and are triggered by divalent cation concentrations similar to those which cause functional uncoupling, strengthening the hypothesis that they are closely related to the mechanism which modulates gap junction permeability.

The data from the calcium ionophore experiments indicate clearly that an increase in $[Ca^{++}]_i$ is paralleled by a tightening and crystallization of particle packings in gap junctions, but do not answer whether the junctional crystallinity is a direct or mediated calcium effect. In fact, in intact cells, changes in $[Ca^{++}]_i$ are expected to promote a variety of events affecting different parameters of the intracellular homeostasis, including enzyme activity and pH (23), hence, it would be impossible to decide whether or not the junctional changes and possibly the functional uncoupling are due to a direct interaction between the suspected uncoupling agents and the channel structures. The main advantage in using isolated junctions is that it allows one to test individually and more directly the effects of the postulated uncoupling agents on the junctional molecules.

Calcium affects isolated lens junctions at a concentration as low as $5 \cdot 10^{-7}$ M. This value is quite reliable since the Ca^{++} buffering capacity of EDTA is substantial within a $[Ca^{++}]$ range of 10^{-8}–10^{-6} M (Fig. 1). However, whether or not similar $[Ca^{++}]$ values trigger particle crystallization in junctions of intact cells is uncertain, as there are reasons to believe that other cations such as Na^+, K^+, and H^+ may affect in a competitive way the Ca^{++} sensitivity of gap junctions (31, 32). Interestingly, gap junction architectural changes occur rather abruptly at a $[Ca^{++}]$ between 3 and $5 \cdot 10^{-7}$ M, indicating that some cooperativity among the particles may exist.

A curious finding is the presence of loosely packed junctional regions frequently intermixed with crystalline packings in both Ca^{++}- and Mg^{++}-treated junctions. This could result from the inaccessibility of these regions to Ca^{++} and Mg^{++} because of their close apposition to other membranes, the possible loss of junctional components necessary for particle crystallization during the junction isolation procedure (16), the interruption of the crystallization process still incomplete at the time of fixation, or other. The process of particle packing is likely to start simultaneously in different regions of the same junctions, expanding radially from nuclei of crystallization. This is suggested by the observation of junctions containing disklike patches of crystallinity surrounded by region with disorderly packed particles.

Particle crystallization and the recovery process seem to be energy independent. This indicates that the architectural changes at the junctions and possibly the functional uncoupling are not the product of a complex enzymatic machinery, but rather a simple on-off mechanism driven by binding and unbinding of divalent cations and hydrogen.

TABLE I

Ca^{++} Effects on the Crystallinity of Particle Packing in Isolated Lens Fiber Gap Junctions

$[Ca^{++}]$	Percent of crystalline junctions	No. of junctions studied	No. of experiments performed
$5 \cdot 10^{-7}$ M or higher	89.3	131	13
$3 \cdot 10^{-7}$ M or lower	0.88	114	11

TABLE II

Mg^{++} Effect on the Crystallinity of Particle Packing in Isolated Lens Fiber Gap Junctions

$[Mg^{++}]$	Percent of crystalline junctions	No. of junctions studied	No. of experiments performed
$1 \cdot 10^{-3}$ M or higher	82.1	112	6
$1 \cdot 10^{-4}$ M or lower	4.5	89	8

Magnesium affects the junctions at a concentration much higher than Ca^{++}, but its triggering concentration value could not be defined as precisely as for Ca^{++}. In fact, the Mg^{++} buffering capacity of EDTA is substantial only for a $[Mg^{++}]$ ranging from 10^{-6} to 10^{-4} M (Fig. 1), and EGTA has low affinity for Mg^{++} at pH 7. In these experiments, however, our main concern was to determine whether or not Mg^{++} affects the junctions independently from Ca^{++}. Indeed, the effective Ca^{++} buffering capacity of the solutions employed strongly supports the independent role of Mg^{++}. The effective $[Mg^{++}]$ is probably between $1 \cdot 10^{-3}$ and $5 \cdot 10^{-3}$ M, as preparations treated with $1 \cdot 10^{-3}$ M $[Mg^{++}]$ often gave borderline results, while at $5 \cdot 10^{-3}$ M $[Mg^{++}]$ the crystallization phenomenon was widespread. A variety of values have been reported for the $[Mg^{++}]_i$, ranging from $4 \cdot 10^{-4}$ to $4.4 \cdot 10^{-3}$ M (4, 6, 8, 15, 25, 41). Thus the $[Mg^{++}]$ which affects the junctions is apparently close to the $[Mg^{++}]_i$; however, as discussed for the Ca^{++}, other cytoplasmic cations may compete with Mg^{++} for the junctional sites and possibly raise its threshold concentration.

The successful recovery of the control particle arrangement by removal of divalent cations at pH 7.5 indicates that the crystallization process does not reflect a deterioration of the junctional structure brought about by activation of proteolitic enzymes or others. However, exposure to recovery solutions never resulted in complete recovery as up to 18% of the junctions remained crystalline. Lack of recovery in some junctions could have resulted from the formation of sealed junctional vesicles during Ca^{++}-Mg^{++} exposure, for which some of the junctions may have become inaccessible to recovery solutions, or may reflect a high binding constant of gap junction macromolecules to divalent cations. The latter could be supported by the observation that more successful recoveries can be obtained by raising the pH of the recovery solutions from 7 to 7.5 (the higher the pH the higher the EDTA-Ca^{++} binding constant). To test this hypothesis, recovery experiments are presently under way using *trans*-1,2-diaminocyclohexane tetraacetate (CDTA), a chelator more efficient than EDTA.

The mechanism of particle clumping into crystalline arrays and the possible relationship between crystallinity and changes in channel permeability are still uncertain. Particle clumping could result from the activation of a contractile apparatus associated with the cytoplasmic surface of the junctions. Indeed, microfilaments have recently been demonstrated in close association with various mammalian gap junctions (20); however, microfilaments are only seen at the convex surface of gap junction vesicles or at junctions in the process of being internalized, indicating their possible involvement in the mechanism

of gap junction endocytosis and degradation (20). Our observation of smooth PS surfaces in isolated lens junctions and the absence of cytoplasmic filaments in close association with the cytoplasmic surface of gap junction particles in intact stomach suggest that neither microfilaments nor other cytoskeletal structures are attached to gap junctions which are not undergoing the internalization process. In addition, the energy independency of both crystallization and recovery processes does not support the involvement of a contractile machinery on theoretical grounds. However, the possibility that cytoplasmic ma-

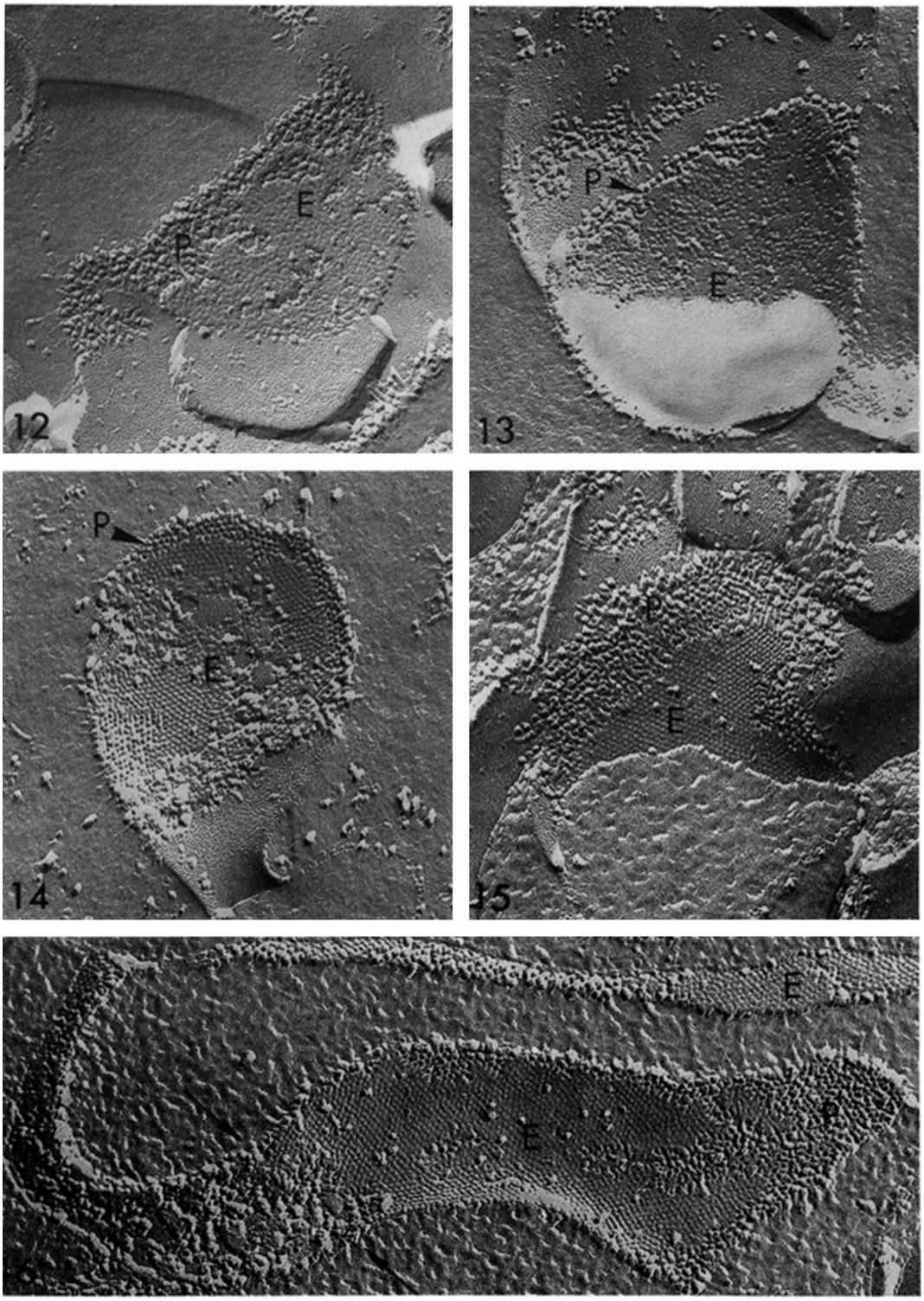

FIGURES 12–16 Freeze-fracture replicas of gap junctions isolated from calf lens fibers, in the presence of EDTA, and subsequently incubated in Ca^{++}-free solutions in which the $[Mg^{++}]$ is $1 \cdot 10^{-5}$ M (Fig. 12), $1 \cdot 10^{-4}$ M (Fig. 13), $1 \cdot 10^{-3}$ M (Figs. 14 and 16), and $5 \cdot 10^{-3}$ M (Fig. 15). Notice that particles and pits form crystalline arrays at $[Mg^{++}]$ of $1 \cdot 10^{-3}$ M or greater (Figs. 14–16), whereas at lower concentrations (Figs. 12 and 13), they remain irregularly aggregated. In some junctions, regions with disorderly packed particles (Fig. 16, left of arrows) are seen in continuity with crystalline areas. *P*, P face, *E*, E face. × 123,600.

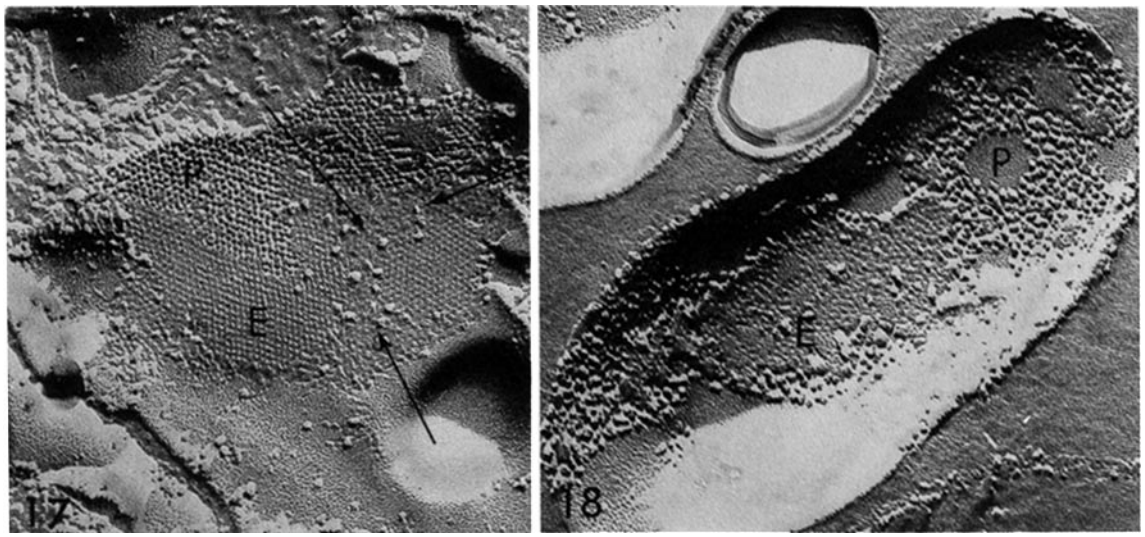

FIGURE 17 Freeze-fracture replica of a gap junction isolated from calf lens fibers, in the presence of EDTA, and subsequently incubated in a solution with a $[Ca^{++}]$ of $1 \cdot 10^{-4}$ M and a $[Mg^{++}]$ of $1 \cdot 10^{-3}$ M. Particles and pits are packed into crystalline arrays. Notice that the junction displays round patches of crystallinity surrounded by regions with disordered arrays (arrows). This suggests that the process of particle crystallization may proceed radially around nuclei of crystallization. *P*, P face; *E*, E face. × 123,600.

FIGURE 18 Freeze-fracture replica of a gap junction isolated in the presence of EDTA, incubated in a solution with a $[Ca^{++}]$ of $1 \cdot 10^{-4}$ M and a $[Mg^{++}]$ of $1 \cdot 10^{-3}$ M and subsequently incubated in a Ca^{++}-, Mg^{++}- free (recovery) solution at pH 7.5. Notice that particles and pits are irregularly packed as in junctions which have not been exposed to divalent cations (Figs. 8, 10, 12 and 13). *P*, P face; *E*, E face. × 123,600.

terial might have been lost from lens junctions during the isolation procedure cannot be discarded.

Particle clumping could result from neutralization of surface charges. Indeed, a number of experimental data seem consistent with this interpretation. Thus, we have proposed as a hypothesis that both the architectural changes in gap junctions and the narrowing of the intercellular channels follow a blockage of negatively charged sites on the junctional proteins (31, 32). Electrophysiological studies indicate that all divalent cations yet tested are effective uncouplers (10–14, 21, 22, 24, 38–40), but they differ in their ability to trigger uncoupling ($Ca^{++} > Mg^{++} > Sr^{++} > Ba^{++}$) (24). Ultrastructural evidence from this and other studies (29–32) indicates that Ca^{++} and Mg^{++} are capable of triggering gap junction particle clumping independently from each other. Also interesting in these studies, Ca^{++} has proven more effective than Mg^{++}. The differences in the effectiveness of the various divalent cations on both gap junction structure and uncoupling suggest differences in their affinity to charged sites on the proteins, which could be explained by steric reasons. Since Ca^{++} is the most effective, its crystalline diameter (~2 Å) (26) could be similar to the size of the protein site. If this were the case, Sr^{++} and Ba^{++} being larger and Mg^{++} smaller than Ca^{++}, their interaction with the proteins would be expected to be somewhat weaker, which would be consistent with their effectiveness at concentrations higher than that of Ca^{++}. Consistent with this hypothesis is the recent finding (14) that La^{3+} uncouples heart cells faster than Ca^{++}. In fact, La^{3+}, having three charges and a crystalline diameter (2.3 Å) (26) very close to that of Ca^{++}, is expected to interact with negatively charged sites even more strongly than Ca^{++}.

Neutralization of negative charges on the cytoplasmic surfaces of the particles would induce the particles to associate tightly into crystalline arrays and would trigger conformational changes in particle protein causing a narrowing of the intercellular channels. Channel occlusion might precede particle crystallization as lipid redistribution, believed to accompany the change in particle packing, is likely to be a relatively slow phenomenon. Indeed, a preliminary report on the effects of exposure to CO_2 indicates that particle movement may lag behind electrical resistance changes, at least in the recovery phase (17).

TABLE III

Recovery from Ca^{++}, Mg^{++} Effect on the Crystallinity of Particle Packing in Isolated Lens Fiber Junctions

	Percent of crystalline junctions	No. of junctions studied	No. of experiments performed
$1 \cdot 10^{-4}$ M $[CA^{++}]$ $1 \cdot 10^{-3}$ M $[Mg^{++}]$	89.7	68	4
EGTA (after CA^{++}, Mg^{++} treatment as above)	17.9	84	5

In conclusion, this study has produced evidence that divalent cations reversibly affect gap junctions by causing the intramembrane particles to clump into crystalline arrays, similarly to uncoupling treatment applied to intact cells. The particle clumping phenomenon, and possibly the narrowing of the channels, are believed to follow a blockage of negatively charged protein sites accessible to divalent cations.

The authors wish to thank Dr. Richard Connett for his collaboration in analyzing ATP.

This research was supported by a grant from the National Institutes of Health (GM 20113).

Received for publication 27 February 1980, and in revised form 17 July 1980.

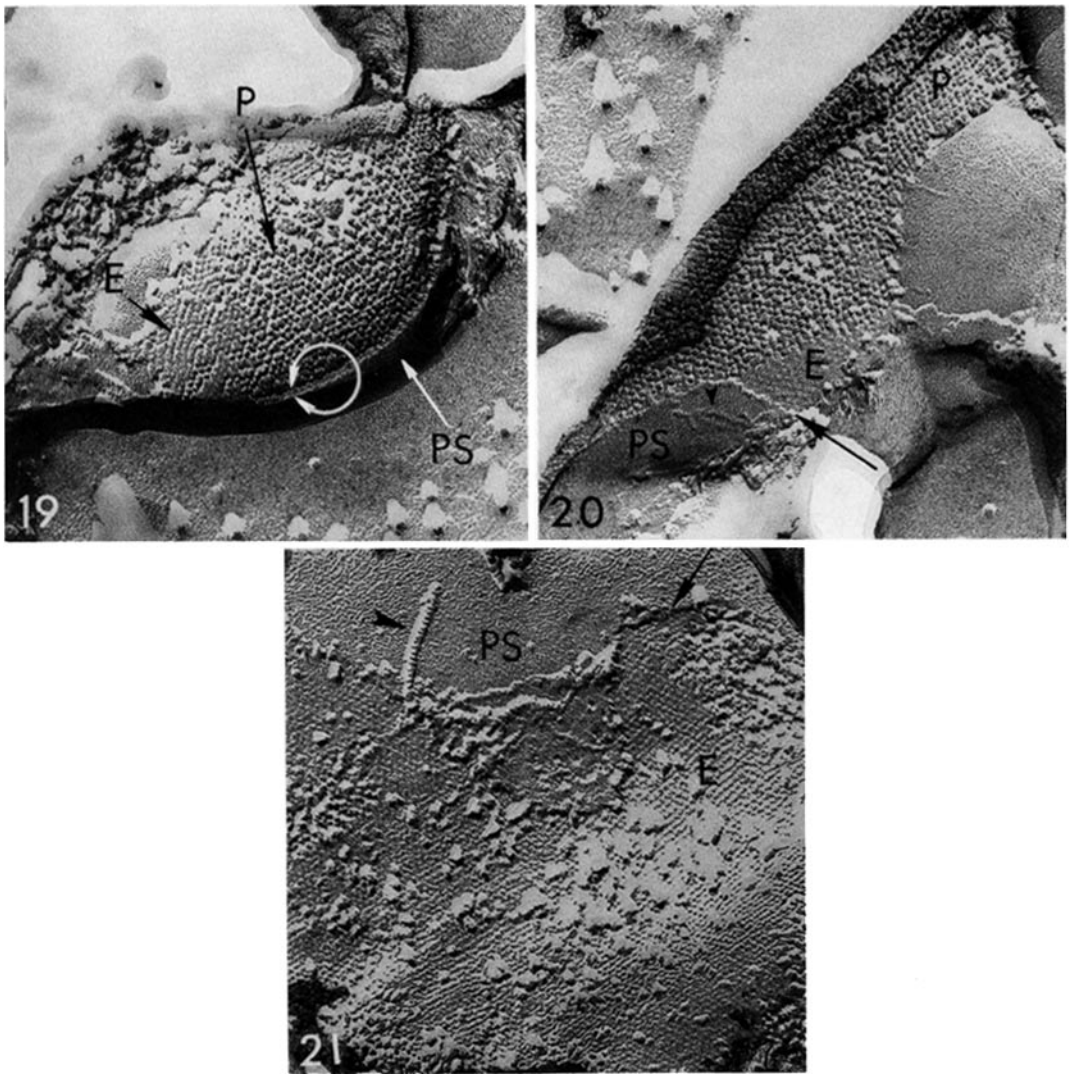

FIGURES 19–21 Replicas of freeze-fractured and deeply etched gap junctions isolated from calf lens fibers, in the presence of EDTA, and subsequently incubated in a Ca^{++}-free solution with a $[Mg^{++}]$ of $1 \cdot 10^{-3}$ M. The true cytoplasmic surface (*PS*) of the junction, exposed by etching, appears mostly smooth. Rarely filamentous structures (Figs. 20 and 21, arrowheads) are seen; one (Fig. 21) could be an intermediate filament as it is ~10-nm thick and has an axial periodicity of 5–6 nm. The double headed arrow of Fig. 19 limits the gap junction thickness comprised between P face and PS surface. In Figs. 20 and 21, the arrows point to those regions where fractured and etched surfaces meet. *P*, P face; *E*, E face. × 123,600.

REFERENCES

1. Baldwin, K. M. 1977. The fine structure of healing over in mammalian cardiac muscle. *J. Mol. Cell Cardiol.* 9:959–966.
2. Baldwin, K. M. 1979. Cardiac gap junction configuration after an uncoupling treatment as a function of time. *J. Cell Biol.* 82:66–75.
3. Benedetti, E. L., I. Dunia, C. J. Bentzel, A. J. M. Vermorken, M. Kibbelaar, and H. Bloemendal. 1976. A portrait of plasmamembrane specializations in eye lens epithelium and fibers. *Biochim. Biophys. Acta* 457:348–353.
4. Berger, J., G.-R. Jänig, G. Gerber, K. Ruckfaul, and S. M. Rapoport. 1973. Interaction of hemoglobin with ions. Interactions among magnesium adenosine 5′-triphosphate, 2,3, Bisphophoglycerate, and oxygenated and deoxygenated human haemoglobin under stimulated intracellular conditions. *Eur. J. Biochem.* 38:553–562.
5. Branton, D., S. Bullivant, N. B. Gilula, M. J. Karnovsky, H. Moor, K. Mühlethaler, D. H. Northcote, L. Packer, B. Satir, V. Speth, L. A. Staehelin, R. L. Steere, and R. S. Weinstein. 1975. Freeze-etching nomenclature. *Science (Wash., D. C.).* 190:54–56.
6. Brinley, F. J., Jr., and A. Scarpa. 1975. Ionized magnesium concentration in axoplasm of dialyzed squid axons. *FEBS (Fed. Eur. Biochem. Soc.) Lett.* 50:82–85.
7. Chaberek, S., and A. E. Martell. 1959. Organic sequestering agents. John Wiley & Sons, New York.
8. Cohen, S. M., and C. T. Burt. 1977. ^{31}P nuclear magnetic relaxation studies of phosphocreatine in intact muscle: determination of intracellular free magnesium. *Proc. Natl. Acad. Sci. U. S. A.* 74:4271–4275.
9. Dahl, G., and G. Isenberg. 1980. Decoupling of heart muscle cells: correlation with increased cytoplasmic calcium activity and with changes of nexus ultrastructure. *J. Membr. Biol.* 53:63–75.
10. Délèze, J. 1965. Electrophysiology of the Heart. B. Taccardi and G. Marchetti, editors. Pergamon Press, Oxford, England. 147–148.
11. Délèze, J. 1970. The recovery of resting potential and input resistance in sheep heart injured by knife or laser. *J. Physiol.* 208:547–562.
12. Délèze, J., and W. R. Loewenstein. 1976. Permeability of a cell junction during intracellular injection of divalent cations. *J. Membr. Biol.* 28:71–86.
13. DeMello, W. C. 1975. Effects of intracellular injection of calcium and strontium on cell communication in heart. *J. Physiol.* 250:231–245.
14. DeMello, W. C. 1979. Effect of intracellular injection of La^{3+} and Mn^{2+} on electrical coupling of heart cells. *Cell Biol. Int. Rep.* 3:113–119.
15. Flatman, P., and V. L. Lew. 1977. Use of ionophore A23187 to measure and to control free and bound cytoplasmic Mg in intact red cells. *Nature (Lond.).* 267:360–362.
16. Goodenough, D. A. 1979. Lens gap junctions: a structural hypothesis for nonregulated low-resistance intercellular pathways. *Invest. Ophthalmol. Vis. Sci.* 18:1104–1122.
17. Hanna, R. B., D. C. Spray, P. G. Model, A. L. Harris, and J. V. L. Bennett. 1978. Ultrastructure and physiology of gap junctions of an amphibian embryo, effects of CO_2. *Biol. Bull.* 155:442(Abstr.).
18. Iwatsuki, N., and O. H. Petersen. 1979. Pancreatic acinar cells: the effects of carbon dioxide, ammonium chloride and acetylcholine on intercellular communication. *J. Physiol. (Lond.).* 291:317–326.
19. Lamprecht, W., and I. Trautshold. 1965. Adenosine-5″-triphosphate. Determination with hexokinase and glucose-6-phosphate dehydrogenase. *In* Methods of Enzymatic Analysis. H. V. Bergmeyer, editor. Academic Press, Inc., New York 543–551.
20. Larsen, W. J., and N.-N. Tung, S. A. Murray, and C. A. Swenson. 1979. Evidence for the participation of actin microfilaments and bristle coats in the internatilization of gap junction membrane. *J. Cell Biol.* 83:576–587.
21. Loewenstein, W. R. 1966. Permeability of membrane junctions. *Ann. N. Y. Acad. Sci.* 137: 441–472.
22. Loewenstein, W. R. 1967. Cell surface membranes in close contact. Role of calcium and magnesium ions. *J. Colloid. Sci.* 25:34–46.
23. Meech, R., and R. C. Thomas. 1977. The effect of calcium injection on the intracellular

sodium and pH of snail neurons. *J. Physiol. (Lond.)*. 265:867–879.
24. Oliveira-Castro, G. M., and W. R. Loewenstein. 1971. Junctional membrane permeability. Effect of divalent cations. *J. Membr. Biol.* 5:51–77.
25. Page, E., and P. Polimeni. 1972. Magnesium exchange in rat ventricle. *J. Physiol. (Lond.)*. 224:121–139.
26. Pauling, L. C. 1960. Nature of the Chemical Bond. Cornell University Press, Ithaca, N. Y.
27. Peracchia, C. 1974. A structure-function correlation in gap junctions of crayfish. Abstracts of 8th International Congress on Electron Microscopy. J. V. Sanders and D. J. Goodchild, editors. The Australian Academy of Sciences, Canberra A.C.T. Australia 2:226–227.
28. Peracchia, C. 1977. Gap junctions: structural changes after uncoupling procedures. *J. Cell Biol.* 72:628–641.
29. Peracchia, C. 1977. Changes in gap junctions with uncoupling are a calcium effect. *J. Cell Biol.* 75(2, Pt. 2): 65 *a*(Abstr.).
30. Peracchia, C. 1978. Calcium effects on gap junction structure and cell coupling. Nature (*Lond.*). 271:669–671.
31. Peracchia, C. 1980. Structural correlates of gap junction permeation. *Int. Rev. Cytol.* 66: 81–146.
32. Peracchia, C., G. Bernardini, and L. L. Peracchia. 1979. Uncoupling mechanism: a hypothesis. *J. Cell Biol.* 83(2, Pt. 2):86 *a*(Abstr.).
33. Peracchia, C., and A. F. Dulhunty. 1974. Gap junctions: structural changes associated with changes in permeability. *J. Cell Biol.* 63(2, Pt. 2):263 *a*(Abstr.).
34. Peracchia, C., and A. F. Dulhunty. 1976. Low resistance junctions in crayfish: structural changes with functional uncoupling. *J. Cell Biol.* 70:419–439.
35. Peracchia, C., and B. S. Mittler. 1972. Fixation by means of glutaraldehyde-hydrogen peroxide reaction products. *J. Cell Biol.* 53:234–238.
36. Peracchia, C., and L. L. Peracchia. 1978. Orthogonal and rhombic arrays in gap junctions exposed to low pH. *J. Cell Biol.* 79(2, Pts. 2):217 *a*(Abstr.).
37. Peracchia, C., and L. L. Peracchia. 1980. Gap junction dynamics: reversible effects of hydrogen ions. *J. Cell Biol.* 87:719–727.
38. Politoff, A., G. D. Pappas, and M. V. L. Bennett. 1974. Cobalt ions cross an electrotonic synapse if cytoplasmic concentration is low. *Brain Res.* 76:343–346.
39. Rose, B., and W. R. Loewenstein. 1975. Permeability of cell junction depends on local cytoplasmic calcium activity. *Nature (Lond.)*. 254:250–252.
40. Rose, B., and W. R. Loewenstein. 1976. Permeability of a cell junction and the local cytoplasmic free ionized calcium concentration: a study with aequorin. *J. Membr. Biol.* 28: 87–119.
41. Tiffert, T., F. J. Brinley, and A. Scarpa. 1977. Ionized magnesium concentration in barnacle muscle fibers. *Biophys. J.* 17:204 *a*(Abstr.).
42. Turin, L., and A. Warner. 1977. Carbon dioxide reversibly abolishes ionic communication between cells of early amphibian embryo. *Nature (Lond.)*. 270:56–57.
43. Turin, L., and A. Warner. 1980. Intracellular pH in early *Xenopus* embryos: its effect on current flow between blastomeres. *J. Physiol. (Lond.)*. 300:489–504.
44. Weingart, R., and W. Reber. 1979. Influence of internal pH on r_i of Purkinje fibers from mammalian heart. *Experientia*. 35:17(Abstr.).
45. Winegrad, S. 1971. Studies of cardiac muscle with a high permeability to calcium produced by treatment with ethylenediaminetetraacetic acid. *J. Gen. Physiol.* 58:71–93.